Design and synthesis of new cell penetrating peptides: Diffusion and distribution inside the cornea

Design and synthesis of new cell penetrating peptides: diffusion and distribution inside the cornea

Silvia Pescina[a*], Marina Sala[b*], Cristina Padula[a], Maria Carmina Scala[b], Antonia Spensiero[b], Silvana Belletti[c], Rita Gatti[c], Ettore Novellino[d], Pietro Campiglia[b], Patrizia Santi[a], Sara Nicoli[a], Carmine Ostacolo[d**]

[a] Department of Pharmacy, University of Parma, Parco Area delle Scienze 27/A, 43124 Parma, Italy

[b] Department of Pharmacy, University of Salerno, Via G. Paolo II 132, 84084 Fisciano (SA), Italy

[c] Department of Biomedical, Biotechnological and Translational Sciences, University of Parma, Via Volturno 39, 43126 Parma, Italy

[d] Department of Pharmacy, University of Naples Federico II, Via D. Montesano 49, 80131 Napoli, Italy

* These Authors contributed equally to this work

** Corresponding Author

Keywords

penetratin
pep-1
cell penetrating peptides
trans-corneal delivery
confocal microscopy
corneal epithelium
ocular drug delivery

1 Introduction

Cell penetrating peptides (CPPs) are short chain peptides (less than 30 amino acids) of natural, chimeric or synthetic origin and generally bearing a positive charge, able to penetrate cellular membranes [1]. The mechanism of cellular internalization is not completely understood: multiple pathways have been described, involving endocytosis (clatrin or caveolae mediated) or direct translocation through the formation of inverted micelles or transient trans-membrane pores [1]. The mechanism depends upon peptide sequence (i.e. amino acid units/residuals, hydrophobicity, total charge), experimental conditions and cell type [2], and more than one mechanism is probably involved. Thanks to this intrinsic penetration ability and low toxicity, CPPs have been proposed as carriers to deliver different kinds of "cargo" to cells, where the cargo is represented by therapeutic molecules (small drugs, nucleic acids, proteins) or nanocarriers covalently or non-covalently bound [2].

CPPs have also been investigated to promote drug permeation across the skin [3] and across epithelial tissues such as nasal [4], intestinal [5], pulmonary [6] and across ocular tissues for the targeting of both anterior and posterior segments [7] [8] [9].

The enhancement of trans-corneal transport for anterior segment targeting is a very important issue. In fact, the optimisation of drug transport could lead to higher drug availability and a lower instillation frequency with important outcomes on efficacy and patient compliance. Additionally, CCPs could give the opportunity to administer topically molecules with unfavourable penetration properties such as oligonucleotides and proteins. Johnson *et al.*, for instance, demonstrated in a murine model the capability of a penetrating peptide (POD) to carry green fluorescent protein in the corneal epithelium [9].

The aim of the work was the design and synthesis of new CPPs and the comparison of their diffusion behaviour and distribution inside the cornea. Starting from the chemical structure of PEP-1 peptide, a well-known CPP [10] 6 mimotopic analogues were designed. The newly synthesized CPPs were labeled with carboxyfluorescein, to make them fluorescent. Using a validated *ex vivo* method (Pescina, Govoni et al. 2015) the ability of CPPs to diffuse through full thickness pig cornea was checked, while a confocal approach was set–up to study peptide localization in the different layers

of the viable epithelium. PEP-1 was used as reference compound while penetratin (PNT) was used as positive control, because of its ability to easily permeate corneal epithelium [8]. Newly synthesized peptides showed corneal accumulation similar or higher than PEP-1 and, interestingly, the tendency to diffuse by a paracellular route. On the contrary, while permeating to a higher extent through the cornea, PNT diffuses by intracellular route, evidencing a different accumulation between wings and basal epithelial cells, probably depending on the stage of cell development.

2 Materials and methods

2.1 Materials

N^{α}-Fmoc-protected amino acids, Rink amide-resin, HOAt, HOBt, HBTU, DIEA, piperidine and trifluoroacetic acid were purchased from Iris Biotech (Germany). Rink Amide-ChemMatrix resin was purchased from Biotage AB (Sweden). Peptide synthesis solvents, reagents, as well as CH_3CN for HPLC were reagent grade and were acquired from commercial sources and used without further purification unless otherwise noted. 5(6)-carboxyfluorescein (5-FAM; mixture of isomers, 97%; MW 376.3 g/mol) was from Alfa Aesar (Karlsruhe, Germany); propidium iodide (PI; MW 668.4 g/mol) from Sigma Aldrich. Phosphate Buffered Saline (PBS) composition: 0.19 g/l KH_2PO_4, 2.37 g/l Na_2HPO_4, 8.8 g/l NaCl; pH 7.4 by adding 85% H_3PO_4. All other materials were of analytical grade.

2.2 Peptide synthesis

The synthesis of PEP-1 mimotopic analogues (**2-7**) was performed according to the solid phase approach using standard Fmoc methodology in a manual reaction vessel [11 12].

The first amino acid, N^{α}-Fmoc-Xaa-OH (Xaa = Trp(Boc), Gln(Trt), Lys(Boc), Val), was linked on to Rink amide resin (0.150 g, loading 0.59 mmol/g) previously deprotected by a 25% piperidine solution in DMF for 30 min. The following protected amino acids were then added on to the resin stepwise. Each coupling reaction was accomplished using a 3-fold excess of amino acid with HBTU and HOBt in the presence of DIEA (6 eq.). The N^{α}-Fmoc protecting groups were removed by treating the protected peptide resin with a 25% solution of piperidine in DMF (1 × 5 min and 1 × 25 min). The peptide resin was washed three times with DMF, and the next coupling step was

initiated in a stepwise manner. The peptide resin was washed with DCM (3×), DMF (3×), and DCM (3×), and the deprotection protocol was repeated after each coupling step. In addition, after each step of deprotection and after each coupling step, Kaiser test was performed to confirm the complete removal of the Fmoc protecting group, respectively, and to verify that complete coupling has occurred on all the free amines on the resin. The N-terminal Fmoc group was removed as described above and resin-bound peptides were reacted with 3 equiv of 5(6)-carboxyfluorescein, N,N'-diisopropyl carbodiimide, and 1-hydroxybenzotriazol, each in DMF for 16h in 10-mL syringes on a shaker at RT. Reactions were stopped by washing the resins three times each with DMF, methanol, dichloromethane, and diethylether. Completeness of N-terminal acylation was confirmed using the Kaiser test.

Finally the peptides were released from the resin with TFA/TIS/H_2O (90:5:5) for 3 h. The resin was removed by filtration, and the crude peptide was recovered by precipitation with cold anhydrous ethyl ether to give a white powder and then lyophilized.

2.2.1 Microwave peptides synthesis

PEP-1 and **PNT** were synthesized using an Automated Microwave Peptide Synthesizer from Biotage AB (Initiator + Alstra™). Peptides were synthesized on a Rink-Amide-ChemMatrix resin (0.150 g, loading 0.3 mmol/g).

The first amino acid, N^{α}-Fmoc-Xaa-OH (Xaa = Val and Lys(Boc)), was linked on to the resin, using as coupling reagent HBTU (3eq, 0.6M), HOAt (3eq, 0.5M) and DIEA (6eq, 2M) in N-methyl-2-pyrrolidone (NMP) [13]. The N^{α}-Fmoc protecting groups were removed by treating the protected peptide resin with a 25% solution of piperidine in DMF (1 × 3 min, 1 × 10 min) at room temperature. The resin was then washed with DMF (4 x 4.5 ml). The following protected amino acids were then added on to the resin stepwise.

Coupling reactions were performed using N^{α}-Fmoc amino acids (3.0 eq., 0.5 M), using as coupling reagent HBTU (3eq, 0.6M), HOAt (3eq, 0.5M) and DIEA (6eq, 2M) in N-methyl-2-pyrrolidone (NMP). All couplings were achieved for 10 min at 75 ºC (2x) and 2x45 min at RT for histidine and cysteine couplings to avoid the epimerization. After each coupling step, the Fmoc

115 protecting group was removed as described above. The resin was washed with DMF (4 × 4.5 ml)
116 after each coupling and deprotection step. Finally peptides were released as described above.

117 **2.2.2 Purification and characterization**

118 All crude peptides were purified by RP-HPLC on a preparative C18-bonded silica column
119 (Phenomenex Jupiter 100 proteo 90Å, 100 x 21.20mm, 10µm) using a Shimadzu SPD 10A
120 UV/VIS detector, with detection at 210 and 254 nm. The column was perfused at a flow rate of 3
121 ml/min with solvent A (10%, v/v, water in 0.1% aqueous TFA), and a linear gradient from 10 to
122 90% of solvent B (80%, v/v, acetonitrile in 0.1% aqueous TFA) over 40 min was adopted for
123 peptide elution. Analytical purity and retention time (tr) of each peptide were determined using
124 HPLC conditions in the above solvent system (solvents A and B) programmed at a flow rate of
125 1.500 ml/min using a linear gradient from 10 to 90% B over 15 min, fitted with C-18 column
126 Phenomenex, Aeris XB-C18 column (150 mm x 4.60, 3.6µm). All analogues showed >97% purity
127 when monitored at 215 nm. Homogeneous fractions, as established using analytical HPLC, were
128 pooled and lyophilized. Peptides molecular weights were determined by ESI mass spectrometry
129 and LC-MS in a LC-MS 2010 instrument fitted with Phenomenex, Aeris XB-C18 column (150 mm
130 x 4.60, 3.6µm), eluted with a linear gradient from 10% to 90% B over 15 min, at a flow rate of
131 1.000 mL/min. ESI-MS analysis in positive ion mode, were made using a Finnigan LCQ Deca ion
132 trap instrument, manufactured by Thermo Finnigan (San Jose, CA, USA), equipped with the
133 Excalibur software for processing the data acquired. The sample was dissolved in a mixture of
134 water and methanol (50/50) and injected directly into the electrospray source, using a syringe
135 pump, which maintains constant flow at 5 ml/min. The temperature of the capillary was set at
136 220°C.
137
138 Table 1. Sequence and analytical data of synthesized peptides.
139

Peptide	Sequence	HPLC	ESI MS	Calc net charge at pH 7
		k'	Calc.	
PEP-1	5FAM-KETWWETWWTEWSQPKKKRKV	3.43	3205.28	+3
pep-2	5FAM-GGKETWWETW	3.27	1636.43	-1
pep-3	5FAM-GGWWETWWTE	3.43	1694.44	-2

pep-4	5FAM-GGTWWTEWSQ	3.59	1594.40	-1
pep-5	5FAM-GGTEWSQPKK	2.57	1474.62	+1
pep-6	5FAM-GGSQPKKKRK	3.24	1470.36	+5
pep-7	5FAM-GGKKKRKV	2.22	1257.52	+5
PNT	5FAM-RQIKIWFQNRRMKWKK	2.89	2602.65	+7

k' [(peptide retention time – solvent retention time)/solvent retention time].
All peptides are amidated at C-terminal.

2.3 Permeation experiments

Permeation studies were carried out through isolated porcine cornea, as previously described [14]. Briefly, porcine corneas were separated from fresh pig eyes (breed, Large White and Landrace; weight: 145-190 kg; age: 10-11 months) and mounted on Franz-type diffusion cells (permeation area of 0.2 cm^2) with the epithelial side facing donor compartment. As donor solution, 200 µl of 5-FAM or CPPs dissolved in PBS was used. Donor concentration for 5-FAM was 2 mg/ml, while in case of CPPs different concentrations (between 0.14 and 0.41 mg/ml – see Table 2) were used. The concentration selected was linked to the sensitivity of the analytical method and permeability of the single CCPs.

The receptor compartment was filled with *approx* 4 ml of degassed PBS, constantly mixed and kept at 37°C. Over the course of experiments (8 hours), 200 µl of the receptor fluid were collected and immediately replaced with fresh PBS. Permeation samples were analysed using an Infinite F200 microplate reader (Tecan Trading AG, Switzerland) set at λ_{ex} 485 nm and λ_{em} 535 nm. Standard solutions were prepared in PBS. Interval of calibration curves was 2.5-100 ng/ml for 5-FAM, while 50-1000 ng/ml for CPPs; RSD% (relative standard deviation %) and ER% (relative error %) resulted lower than 5% and 10% respectively for all the concentrations tested.

The data was plotted as amount of 5-FAM or CPP permeated (µg/cm^2) as a function of time (min); the trans-corneal flux (J, µg/cm^2 min) was determined as the slope of the regression line at steady state, while the apparent permeability coefficient (P_{app}, cm/s) was calculated at the steady state as:

$P_{app} = J/C_D$ **equation 1**

being C_D (µg/ml) the concentration of the donor solution.

2.4 Confocal microscopy

For confocal microscopy studies, eye bulbs kept in a media for corneal storage (EUSOL-C, Alchimia, Padova, Italia) or PBS at 4°C, were used within 2 hours from enucleation. The cornea was dissected, a 0.6 cm^2 corneal disc was punched in the center of the cornea and incubated with PNT (25 µg/ml), PEP-1 (3 mg/ml) or pep-7 (2.4 mg/ml) at room temperature for 1h. The incubation was performed using a special flow chamber expressly designed for confocal observations [15]. 100 µl of CPPs solution was inserted at the bottom of the cell and the corneal disc was applied with the epithelial side facing the solution: with this apparatus (Figure 1) CPPs can diffuse across the epithelium, but can also penetrate via lateral side, allowing for a faster contact with the different epithelial layers. Analysis was performed using LSM 510 Meta confocal system scan integrated with Axiovert 200M inverted microscope (Carl Zeiss, Jena , Germany). Samples were observed through a 40x, 1.3 NA oil objective. 5-FAM and PI were excited with 488 nm argon and 543 nm He-Ne laser lines, respectively. Image acquisition was carried out with relevant beamsplitter and emission recorded through 505-530 BP filter for 5-FAM and 560 LP filter for PI. A series of x-y sections were acquired with a z-step of 1µm to cover the whole height of samples. For 3D reconstruction, stacks of digital images were processed employing the “transparency” algorithm of the “Inside 4D” module of Axiovision (release 4.5) software (Carl Zeiss, Jena Germany).

The set-up of the method was done using a formalin-fixed porcine cornea stained with propidium iodide (PI). Briefly, the tissue was fixed for 24 h in 10% buffered formalin and then permeabilized with 80% ethanol. Tissue was then stained with 1µg/ml PI solution for 30 minutes and then observed with confocal microscope. A sample of fresh cornea was stained immediately after dissection with the same solution to provide a test for tissue viability. Propidium iodide is a red fluorescent nuclear dye, which simultaneously provides a good fluorescent dye for nuclear morphology and a vital probe to assess cell viability.

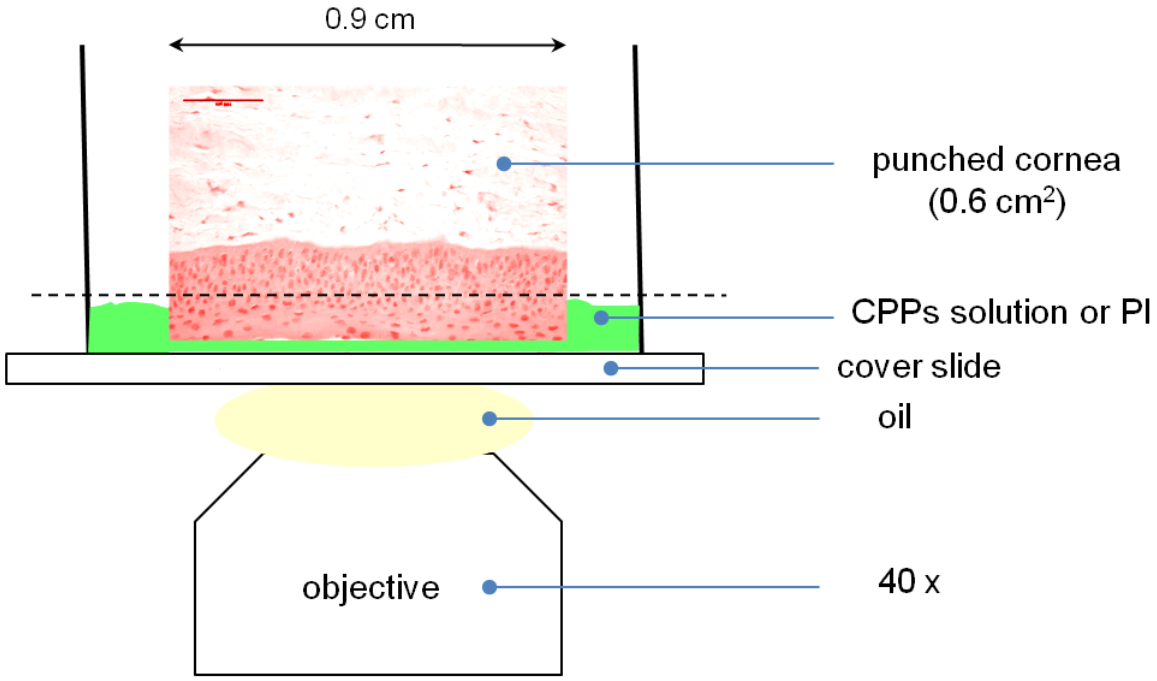

Figure 1. Experimental set-up used for confocal microscopy studies.

3 Results and Discussion

3.1 Design

Starting from PEP-1 we designed a small library of overlapping peptides, with a specific length and specific offset, to cover the entire PEP-1 sequence as shown in Figure 2. The synthesis of seven short fluorescein labeled peptides was attempted but (Table 1), unfortunately, we were not able to obtain peptide 3 (pep-3) in sufficient yield to test. To avoid influence of fluorescein group on peptides structure, a glycine spacer was inserted in the sequences. We also synthesized PEP-1 as reference compound and Penetratin (PNT) as control.

KETWWETWWTEWSQPKKKRKV **PEP-1**
KETWWETW
WWETWWTE
TWWTEWSQ
TEWSQPKK
SQPKKKRK
KKKRKV

Figure 2. Overlapping peptides library.

3.2 Trans-corneal permeation

The CPPs synthesised in the present work were labelled with 5-FAM, a low molecular weight (376.32 g/mol) highly hydrophilic and negatively charged molecule ($LogD_{7.3}$ -3.15 [16], charge at pH 7.4 approx. -3 [17]) to make them fluorescent; the trans-corneal permeation of the label 5-FAM was evaluated at first. The permeation profile is reported in Figure 3 Panel a, and the permeability coefficient, calculated using Equation 1, resulted *approx.* $0.3*10^{-6}$ cm/s (Table 2), value similar to that of fluorescein [18] [14], molecule of comparable molecular weight.

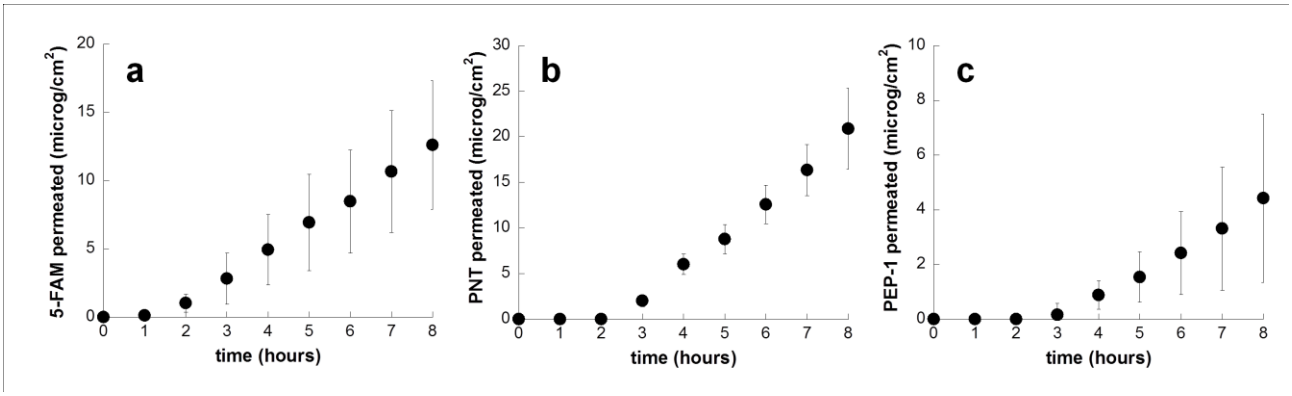

Figure 3. Permeation profiles across isolated porcine cornea of 5-FAM (donor 2 mg/ml) (a), PNT (179.26 µg/ml) (b) and PEP-1 (359.51 µg/ml) (c) solutions. (Mean values±sd)

PNT, despite the high molecular weight (2600 Dalton), considerable hydrophilicity (measured logP -2.1 [19]) and positive charge, permeated the cornea easily (Figure 3, Panel b) and the permeability coefficient resulted 20-fold higher than 5-FAM (Table 2).

Table 2. Apparent permeability coefficients of 5-FAM labelled CPPs and 5-FAM calculated using Equation 1 (mean values±sd)

Permeant (all CPPs were 5-FAM labelled)		**Donor concentration (µg/ml)**	**$P_{app}*10^{-6}$ (cm/s)**
CPPs	*PNT*	179.26	6.18±1.46
	PEP-1	359.51	0.75±0.56**
	pep-2	413.58	1.52±1.36*
	pep-4	146.60	2.00±1.41*
	pep-5	410.09	0.66±0.29**
	pep-6	369.75	0.51±0.06*
	pep-7	344.16	0.71±0.28**
5-FAM		2000.00	0.29±0.08**

* statistically different from PNT, p<0.05 (Student's t test) ** statistically different from PNT, p<0.01 (Student's t test)

The permeation properties of 5-FAM-labelled PNT were previously investigated by Liu *et al.* [8] across isolated rabbit cornea and the permeability coefficient found (10.5±2.20)* 10^{-6} cm/s) is in good agreement with the present data. The good penetration properties of PNT, the third helix of the Antennapedia homeodomain, can be attributed to its capability to interact with and penetrate across cell membranes [20, 21 22].

Also PEP-1 is known to be able to penetrate into HeLa cells [23] although, unexpectedly, its permeability across the cornea was 8 fold lower than PNT (Table 2) and the permeation profile is characterised by a significantly longer lag time (Figure 3). The differences observed between PNT and PEP-1 reflect differences in the permeation across the epithelium: in fact, the permeability coefficient across de-epithelised cornea (i.e. stroma+endothelium) was similar for the two peptides, 17.7±8.5*10^{-6} cm/s in case of PNT and 12.9±3.4*10^{-6} cm/s for PEP-1. These values are comparable to the ones found for the neutral 4.4 kDa dextran and a negatively charged 8 kDa ssDNA, across the same de-epithelized tissue [24]: the possible interaction of the peptides (both positively charged) with GAGs (negatively charged), and in particular with N-linked GAGs [25] highly represented in the extracellular matrix of the cornea [26], did not markedly hinder CPPs diffusion across the corneal stroma.

The newly synthesised peptides (pep-2; pep-4; pep-5; pep-6; pep-7), were evaluated across the intact cornea and the permeability coefficient found resulted similar to the reference PEP-1 (Table 2); the data are characterized by a high variability probably due to their propensity to aggregate in aqueous solution [23, 27]. In particular the highest variability was found for the negatively charged peptides pep-2 (CV% 90) and pep-3 (CV% 70).

No correlation was found between peptide permeability and molecular weight (Figure 4a), surface net charge (Figure 4b) nor charge/mass ratio (Figure 4c).

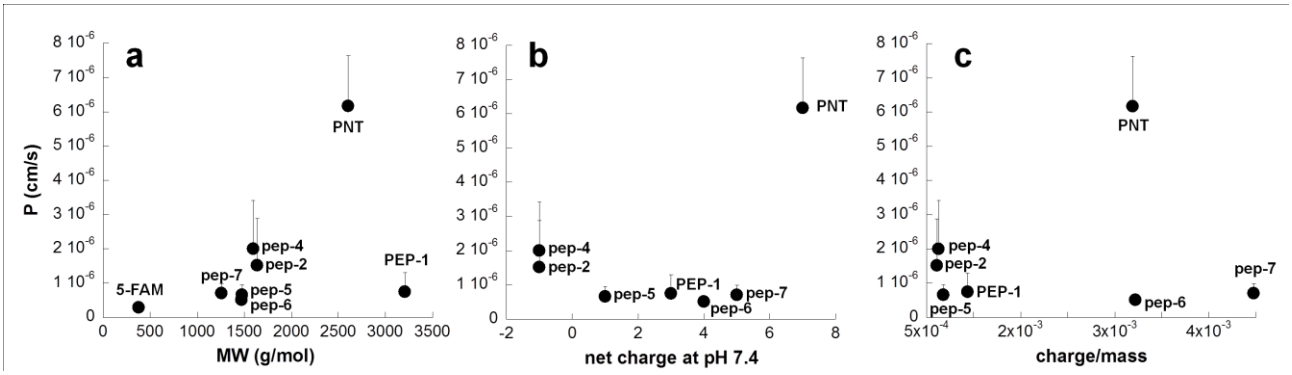

Figure 4. Permeability coefficients of peptides as function of MW (a), net charge (b) and charge/mass ratio (c). (Mean values+sd)

Even if the permeability of peps 1-7 is not as high as PNT, it is comparable to that of PEP-1. Additionally, the permeability is comparable or in some cases higher (pep-7, $p<0.05$) to that of 5-FAM, suggesting that the amphipathic nature and the lower negative charge of peptides counterbalanced the increase in molecular weight.

3.3 Confocal microscopy studies on freshly enucleated pig eyes

Permeation experiments have demonstrated the ability of CPPs to cross the corneal epithelium; the aim of confocal microscopy was then to evaluate the ability of CPPs to enter inside corneal cells. This aspect is very important, since CPPs cell uptake is strictly linked not only to cell type, but also to cell environment that can influence, on one side, the expression of glycosaminoglycans and lipids on cell membranes [2] and, on the other side, the conformation and activity of CPPs [28].

Corneal epithelium is a stratified, squamous, non keratinized tissue; the similarity between porcine and human corneas, in terms of histology and permeability, has been recently demonstrated [14].

Figure 5 shows 3D reconstruction of formalin-fixed (a) and vital (b) corneal epithelium. In the fixed sample, nuclei of the entire epithelial layer (surface, wing, basal cells) are stained by propidium iodide, while in the viable tissue (b) only the superficial cell layer shows PI positive nuclei. PI is excluded from competent plasma membrane (live cells), while is loaded from cells that have lost this competence after cell death (apoptosis and/or necrosis or death after fixation).

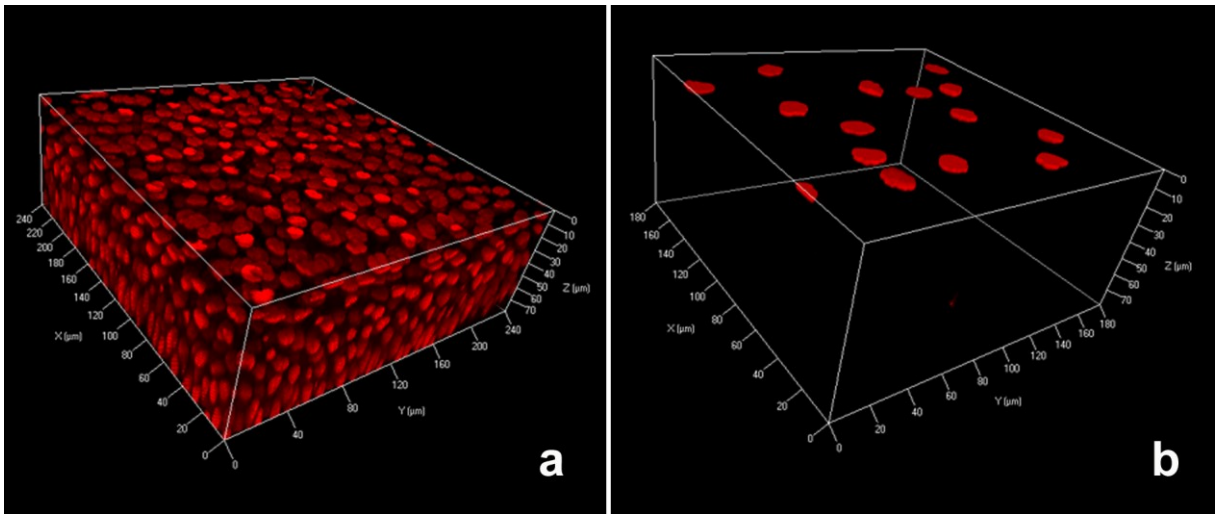

Figure 5. 3D reconstruction of a fixed (**a**) and viable (**b**) corneal epithelium after nuclear staining with PI. Panel **a**: nuclei of the entire epithelial layer (surface, wing and basal cells) are PI positive. Panel **b**: Only superficial cell layer shows PI positive nuclei (dead cells). All underlying cells exclude PI thus are still viable. (z axis represents vertical scanning axis and is *approx*. 80 µm; 0 µm corresponds to superficial layer).

The death of the most external layer can be attributed to the procedure of isolation and transport of eye bulbs, since the epithelium natural turn-over generally occurs through the shedding of isolated dead cells, replaced by underlying viable cells [29]. However, in response to superficial cell death, the sub-surface cells start to develop tight-junctions within minutes; this has been demonstrated to occur also *ex vivo* after the induction of a whole layer of devitalized cells [30]. It has been shown that this process remains active even after keeping the excised cornea for three days in a nutrient medium [30]. These considerations support the reliability of the permeation data obtained in the present work, taking also into account that they are comparable with data found in the literature for both low [14] and high [24] molecular weight compounds.

Confocal analysis of freshly explanted porcine corneas was then performed after contact with either 5-FAM labelled pep-7, PEP-1 or PNT solutions. PNT was used as positive control CPP, PEP-1 as the reference (net charge +3) while pep-7 (net charge +5) was chosen as representative, most promising, peptide among those newly synthesised. The solutions of CPP were left in contact with the cornea for 1 h before confocal analysis. Confocal sections and 3D reconstructed images are reported in Figure 6 and 7, respectively.

Owing to the possibility of interaction (and artefact generation) of propidium iodide with the peptide bound 5-FAM, the marker for cell death was not used, and only the fluorescence of the peptides was observed.

Figure 6 shows confocal sections after 5-FAM-labelled CCPs contact with the corneal tissue. In the case of pep-7, fluorescence is localised only in the intercellular spaces both in wing and in basal epithelial cells, suggesting that the peptide diffuses across the corneal epithelium following the paracellular route. The paracellular route is probably the main diffusion pathway also for PEP-1, although in this case some diffusion across the cellular membrane cannot be completely excluded. In contrast, PEP-1 is reported as capable of entering the cell nucleus of different cells, including human fibroblasts, in less than 10 minutes [31]. In the case of pep-7, no literature data are present but its sequence is shorter and less hydrophobic than PEP-1, lacking of spacer domains as well as of the complete nuclear localization sequence (NLS), and this can contribute to explain its behaviour. Noticeably, promotion of ophthalmic active ingredients (especially peptides) trough the paracellular pathway has gained increasing interest in recent years. Intercellular spaces are, in fact, devoid of the massive intracellular metabolic activity, thereby minimizing the enzymatic penetration barrier [32]. Permeation of hydrophilic compounds is however limited to the small paracellular pores and regulated by the tight junctions. Thus, increasing molecular size of the permeant progressively decreases the rate of permeation [33]. Moreover, one of the main limit associated to the use of CPPs as absorption enhancer is represented by their sensitivity to proteolysis [34]. Limiting the contact with proteolytic enzymes could be a fruitful strategy in increasing their effectiveness.

The result obtained with PNT is completely different. In wing cell layer, the fluorescence is localised in the intercellular space and is characterized by the presence of spots (Figure 6) that, for size and localization, could be attributed to endocytic organelles. Basal cells are clearly fluorescent both inside cytoplasm and nucleus (Figure 6). Apparently, PNT behaves differently depending on the degree of cell maturation. This result is in line with the significant changes taking place in corneal epithelial cells, that from the basal membrane migrate toward the surface loosing proliferative capacity and acquiring features specific for each layers, differing for glycoconjugate composition [30].

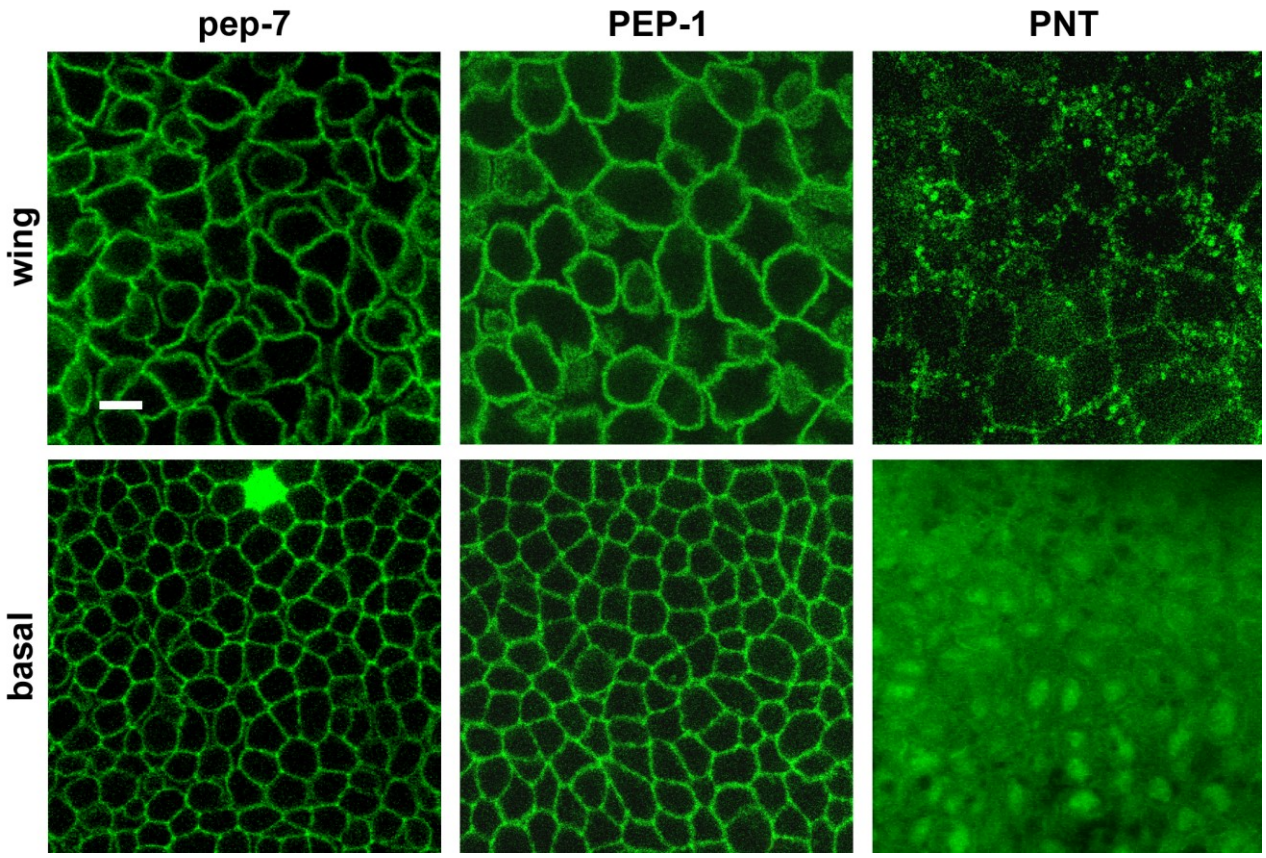

Figure 6. Confocal sections of vital corneal epithelium after incubation with pep-7, PEP-1 and PNT. Images of the first line shows confocal planes acquired from wing layers (cells mean diameter *approx.* 20 µm); images of the second line are planes from basal layers (mean cell diameter *approx* 10 µm). Pep-7 fluorescence distribution is mainly localised outside cells in both layers; pep-7 freely diffuses across the membrane of one dead basal cell that appears green fluorescent. Distribution of PEP-1 in wing and basal layers: fluorescence is mainly extracellular and surrounds cells, also if slight intracellular areas are present in some cells in both layers. PNT shows a spot localization on plasma membrane in wing layer, while localization in basal layers is diffused across cytoplasm and nucleus. (Scale bar:10 µm).

Figure 7 shows 3D reconstruction obtained by processing the stacks of the digital images. The outer layers (0-10 µm depth) are fluorescent due to the loss of integrity of cellular membrane (as previously discussed). 3D images of pep-7 and PEP-1 show clearly their intercellular localization. In the case of PNT, the intermediate layers (containing some surface cells and all wing cells; depth 10-60 µm) show a light fluorescence, mainly localized within the extracellular space, while basal cells (60-80 µm depth) are fluorescent.

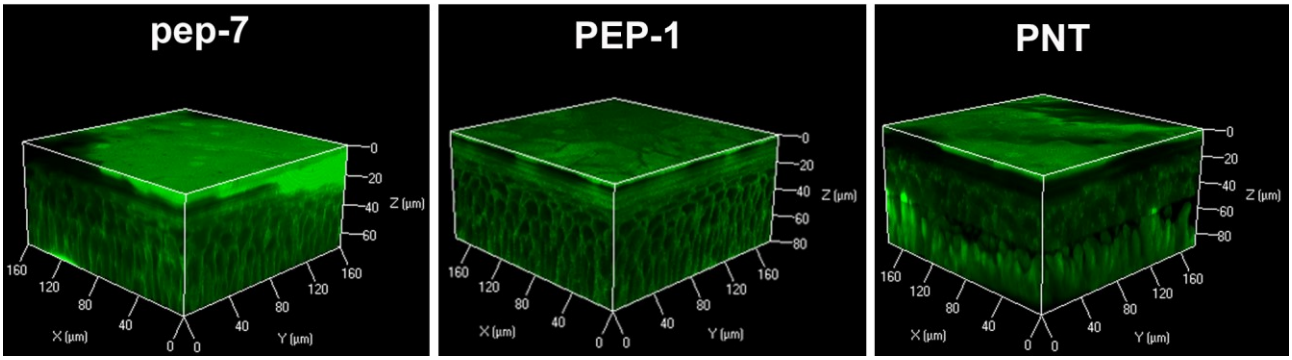

Figure 7. 3D reconstruction of vital corneal epithelium after loading 5-FAM labelled PNT, PEP-1 and pep-7.

4 Conclusion

The mimotopic approach proposed in the present work for the design of novel CPPs proved to be a suitable strategy allowing for the synthesis of shorter and more affordable sequences, with penetration ability comparable to PEP-1, chosen as long-sequence reference peptide. Although none of peptides was able to equal the performance of PNT, used as positive control, a preferential paracellular penetration route was evidenced trough the ocular tissue for PEP-1 and pep-7, highlighting their potential application as specific absorption promoters for metabolic sensitive ophthalmic drugs.

The confocal method developed, allowing for the localization the peptides in the different epithelium layers by studying cell uptake on a 3D complex tissue, also revealed a clear cellular uptake in the case of PNT. An interesting observation is also the different PNT behavior depending on the degree of cell maturation: this result highlights the importance of studying CPPs uptake in conditions as close as possible to the real in vivo condition.

Acknowledgments

The authors want to thank Dott. Pierugo Cavallini and Macello Annoni S.p.A. (Busseto, Parma, Italy) for kindly providing porcine eyes. The confocal images were obtained in the Laboratory of Confocal Microscopy of the S.Bi.Bi.T Department of the University of Parma. The financial support of Italian Ministry of Education, University and Research (PRIN2010H834LS) is gratefully acknowledged.

362

5 References

1. Bechara, C.; Sagan, S. Cell-penetrating peptides: 20 years later, where do we stand? *FEBS Letters* **2013,** *587*, (12), 1693-1702.
2. Copolovici, D. M.; Langel, K.; Eriste, E.; Langel, U. Cell-penetrating peptides: design, synthesis, and applications. *ACS Nano* **2014,** *8*, (3), 1972-94.
3. Nasrollahi, S. A.; Taghibiglou, C.; Azizi, E.; Farboud, E. S. Cell-penetrating peptides as a novel transdermal drug delivery system. *Chemical biology & drug design* **2012,** *80*, (5), 639-46.
4. Khafagy el, S.; Morishita, M.; Isowa, K.; Imai, J.; Takayama, K. Effect of cell-penetrating peptides on the nasal absorption of insulin. *Journal of controlled release : official journal of the Controlled Release Society* **2009,** *133*, (2), 103-8.
5. Khafagy el, S.; Morishita, M. Oral biodrug delivery using cell-penetrating peptide. *Adv Drug Deliv Rev* **2012,** *64*, (6), 531-9.
6. Patel, L. N.; Wang, J.; Kim, K. J.; Borok, Z.; Crandall, E. D.; Shen, W. C. Conjugation with cationic cell-penetrating peptide increases pulmonary absorption of insulin. *Mol Pharm* **2009,** *6*, (2), 492-503.
7. Sun, Q.; Xu, X. A promising future for peptides in ophthalmology: work effectively and smartly. *Current medicinal chemistry* **2015,** *22*, (8), 1030-40.
8. Liu, C.; Tai, L.; Zhang, W.; Wei, G.; Pan, W.; Lu, W. Penetratin, a potentially powerful absorption enhancer for noninvasive intraocular drug delivery. *Mol Pharm* **2014,** *11*, (4), 1218-27.
9. Johnson, L. N.; Cashman, S. M.; Read, S. P.; Kumar-Singh, R. Cell penetrating peptide POD mediates delivery of recombinant proteins to retina, cornea and skin. *Vision Research* **2010,** *50*, (7), 686-697.
10. Deshayes, S.; Morris, M. C.; Divita, G.; Heitz, F. Cell-penetrating peptides: tools for intracellular delivery of therapeutics. *Cellular and molecular life sciences : CMLS* **2005,** *62*, (16), 1839-49.
11. Stewart, J. M.; Young, J. D., *Solid Phase Peptide Synthesis*. Pierce Chemical Co; 2nd edition Rockford, 1984.
12. Atherton, E.; Sheppard, R. C., *Solid Phase Peptide Synthesis: A Practical Approach*. Oxford University Press 1989.
13. Wang, S. S.; Tam, J. P.; Wang, B. S.; Merrifield, R. B. Enhancement of peptide coupling reactions by 4-dimethylaminopyridine. *International journal of peptide and protein research* **1981,** *18*, (5), 459-67.
14. Pescina, S.; Govoni, P.; Potenza, A.; Padula, C.; Santi, P.; Nicoli, S. Development of a convenient ex vivo model for the study of the transcorneal permeation of drugs: histological and permeability evaluation. *J Pharm Sci* **2015,** *104*, (1), 63-71.
15. Gatti, R.; Orlandini, G.; Uggeri, J.; Belletti, S.; Galli, C.; Raspanti, M.; Scandroglio, R.; Guizzardi, S. Analysis of living cells grown on different titanium surfaces by time-lapse confocal microscopy. *Micron (Oxford, England : 1993)* **2008,** *39*, (2), 137-43.
16. Araie, M.; Maurice, D. The rate of diffusion of fluorophores through the corneal epithelium and stroma. *Experimental eye research* **1987,** *44*, (1), 73-87.
17. Aschi, M.; D'Archivio, A. A.; Fontana, A.; Formiglio, A. Physicochemical properties of fluorescent probes: experimental and computational determination of the overlapping pKa values of carboxyfluorescein. *The Journal of organic chemistry* **2008,** *73*, (9), 3411-7.
18. Stewart, J. M.; Schultz, D. S.; Lee, O. T.; Trinidad, M. L. Collagen cross-links reduce corneal permeability. *Invest Ophthalmol Vis Sci* **2009,** *50*, (4), 1606-12.

19. Lindgren, M. E.; Hallbrink, M. M.; Elmquist, A. M.; Langel, U. Passage of cell-penetrating peptides across a human epithelial cell layer in vitro. *The Biochemical journal* **2004,** *377*, (Pt 1), 69-76.
20. Yesylevskyy, S.; Marrink, S. J.; Mark, A. E. Alternative mechanisms for the interaction of the cell-penetrating peptides penetratin and the TAT peptide with lipid bilayers. *Biophys J* **2009,** *97*, (1), 40-9.
21. Derossi, D.; Calvet, S.; Trembleau, A.; Brunissen, A.; Chassaing, G.; Prochiantz, A. Cell internalization of the third helix of the Antennapedia homeodomain is receptor-independent. *The Journal of biological chemistry* **1996,** *271*, (30), 18188-93.
22. Bahnsen, J. S.; Franzyk, H.; Sandberg-Schaal, A.; Nielsen, H. M. Antimicrobial and cell-penetrating properties of penetratin analogs: effect of sequence and secondary structure. *Biochimica et biophysica acta* **2013,** *1828*, (2), 223-32.
23. Henriques, S. T.; Costa, J.; Castanho, M. A. Re-evaluating the role of strongly charged sequences in amphipathic cell-penetrating peptides: a fluorescence study using Pep-1. *FEBS Lett* **2005,** *579*, (20), 4498-502.
24. Pescina, S.; Govoni, P.; Antopolsky, M.; Murtomaki, L.; Padula, C.; Santi, P.; Nicoli, S. Permeation of proteins, oligonucleotide and dextrans across ocular tissues: experimental studies and a literature update. *J Pharm Sci* **2015,** *104*, (7), 2190-202.
25. Ziegler, A. Thermodynamic studies and binding mechanisms of cell-penetrating peptides with lipids and glycosaminoglycans. *Adv Drug Deliv Rev* **2008,** *60*, (4-5), 580-97.
26. Funderbugh, J. L., The corneal stroma. In *Encyclopedia of the Eye, Four-Volume Set, 1st Edition*, Dartt, D. A., Ed. Elsevier Ltd: 2010.
27. Henriques, S. T.; Castanho, M. A. Environmental factors that enhance the action of the cell penetrating peptide pep-1 A spectroscopic study using lipidic vesicles. *Biochimica et biophysica acta* **2005,** *1669*, (2), 75-86.
28. Eiriksdottir, E.; Konate, K.; Langel, U.; Divita, G.; Deshayes, S. Secondary structure of cell-penetrating peptides controls membrane interaction and insertion. *Biochimica et biophysica acta* **2010,** *1798*, (6), 1119-28.
29. Remington, L. A., *Clinical anatomy and physiology of the visual system*. Third ed.; Elsevier: St. Louis, 2012.
30. Wolosin, J. M.; Xiong, X.; Schutte, M.; Stegman, Z.; Tieng, A. Stem cells and differentiation stages in the limbo-corneal epithelium. *Progress in retinal and eye research* **2000,** *19*, (2), 223-55.
31. Morris, M. C.; Depollier, J.; Mery, J.; Heitz, F.; Divita, G. A peptide carrier for the delivery of biologically active proteins into mammalian cells. *Nature biotechnology* **2001,** *19*, (12), 1173-6.
32. Hämäläinen, K. M.; Kananen, K.; Auriola, S.; Kontturi, K.; Urtti, A. Characterization of paracellular and aqueous penetration routes in cornea, conjunctiva, and sclera. *Invest Ophthalmol Vis Sci* **1997,** *38*, (3), 627-634.
33. Toropainen, E.; Ranta, V. P.; Vellonen, K. S.; Palmgren, J.; Talvitie, A.; Laavola, M.; Suhonen, P.; Hamalainen, K. M.; Auriola, S.; Urtti, A. Paracellular and passive transcellular permeability in immortalized human corneal epithelial cell culture model. *Eur J Pharm Sci* **2003,** *20*, (1), 99-106.
34. Foerg, C.; Merkle, H. P. On the biomedical promise of cell penetrating peptides: limits versus prospects. *J Pharm Sci* **2008,** *97*, (1), 144-62.